Sorafenib promotes graft-versus-leukemia activity in mice and humans through IL-15 production in FLT3-ITD mutant leukemia cells

A full list of authors and affiliations appears at the end of the article.

Abstract

Patients relapsing with FLT3-ITD mutant acute myeloid leukemia (AML) after allogeneic hematopoietic cell transplantation (allo-HCT) have a one-year-survival rate below 20%. We observed that sorafenib, a multi-tyrosine kinase inhibitor, increased IL-15 production by FLT3-ITD^{+}-leukemia cells, which synergized with the allogeneic CD8^{+} T-cell response, leading to long-term survival in six mouse models of FLT3-ITD^{+}AML. Sorafenib treatment-related IL-15 production caused an increase in CD8^{+}CD107a^{+}IFN-γ^{+} T-cells with features of longevity (Bcl-2^{high}, reduced PD-1-levels), which eradicated leukemia in secondary recipients. Mechanistically, sorafenib reduced expression of the transcription factor ATF4, thereby blocking negative regulation of IRF7-activation, which enhanced IL-15 transcription. Both IRF7-knockdown and ATF4-overexpression in leukemia cells antagonized sorafenib induced IL-15 production in vitro. Human FLT3-ITD[+]AML cells of sorafenib-responders obtained post sorafenib-therapy showed increased levels of IL-15, pIRF7, and a transcriptionally active IRF7-chromatin state. Mitochondrial spare respiratory capacity and glycolytic capacity of CD8^{+}T-cells

increased upon sorafenib-treatment in sorafenib-responders but not in non-responders. Our findings indicate that the synergism of T-cells and sorafenib is mediated via reduced ATF4-expression, causing activation of the IRF7/IL-15-axis in leukemia cells leading to metabolic reprogramming of leukemia-reactive T-cells in humans. Sorafenib treatment therefore has the potential to contribute to an immune-mediated cure of FLT3-ITD-mutant AML-relapse, an otherwise fatal complication after allo-HCT.

Introduction

Internal tandem duplications (ITD) of the receptor-tyrosine kinase FLT3 gene are found in 20–25% of acute myeloid leukemias (AML), providing a persistent growth stimulus. Because of the unfavorable prognosis of FLT3-ITD[+]AML, the majority of patients undergoes allogeneic hematopoietic cell transplantation (allo-HCT)[1,2]. Relapse of FLT3-ITD[+]AML after allo-HCT is not curable in the majority of patients. Sorafenib is a multi-tyrosine kinase inhibitor that can reduce proliferation and survival of FLT3-ITD[+]AML cells *in vitro*. While not improving the overall survival (OS) of AML patients when combined with standard-chemotherapy[3,4], sorafenib-treatment caused durable remissions in some patients with FLT3-ITD[+]AML after allo-HCT[5–7] thereby motivating sorafenib-maintenance trials[8–11]. However, the mechanism as to how sorafenib combined with allogeneic immunity may induce long-term control of FLT3-ITD[+]AML remains unknown.

Results

To understand whether functional synergism between allogeneic immune responses and sorafenib occurs, we used a mouse leukemia model[12] that relies on mixed lineage-leukemia-partial-tandem duplication $MLL^{(PTD/wt)}$ and $FLT3^{(ITD/wt)}$-mutations (Fig.1a). Leukemia cells were injected after irradiation/allo-HCT and donor-derived T-cells were infused on day (d) 2 after allo-HCT, analogous to donor lymphocyte infusions (DLI) applied in patients. We observed long-term leukemia-control only in mice receiving both sorafenib and T-cells. Sorafenib was not protective when given alone (Fig.1a). A comparable pattern of leukemia-control was observed in a mouse model of lymphoblastic leukemia (Ba/F3-ITD) with respect to survival (Fig.1b) and expansion of LUC[+]-/GFP[+]-leukemia cells (Fig.1c–e, Suppl.Fig.1a). Microarray-based analysis of Ba/F3-ITD cells revealed that interleukin-15 (*Il-15*) mRNA was upregulated upon sorafenib-exposure in vitro (Fig.1f,g), which was confirmed by qPCR and flow-cytometry (Fig.1h,i). IL-15 production was dependent on sorafenib-sensitivity as Ba/F3-cells expressing the sorafenib-resistant FLT3-ITD[F691L]-mutant showed no increase in IL-15 expression (Fig.1i).

IL-15 increased in the serum of mice that had received T-cells and sorafenib (Fig.1j). Sorafenib-induced serum IL-15 subsided when leukemia cells were reduced (Fig.1j). IL-15 serum levels increased upon FLT3-ITD-inhibition in different mouse myeloid leukemia models (FLT3-ITD-transfected BM, myeloid WEHI-3B[FLT3-ITD] cell line, a genetic AML model that relies on mixed lineage-leukemia-partial-tandem duplication $MLL^{(PTD/wt)}$ and $FLT3^{(ITD/wt)}$-mutations[13]) (Suppl.Fig.1b–d). Sorafenib had no effect on T-cell activation *in*

vitro (Suppl.Fig.1e–h). Leukemia cells expressed IL-15-receptor(R)α (Suppl.Fig.1i,j) which is essential for IL-15 trans-presentation[14].

Genetic deficiency for IL-15 in FLT3-ITD-driven leukemia cells abrogated the beneficial sorafenib effects, while IL-15 deficiency of the recipient did not (Fig.2a,b). Lack of IL-15 in leukemia cells could be rescued by exogenous IL-15 (Fig.2b), however this increased lethality (Fig.2a), due to more severe graft-versus-host disease (GVHD), which was not observed in sorafenib-treated mice (Fig.2c). These data indicate that IL-15 levels made by leukemia cells upon sorafenib-exposure were below a threshold driving GVHD-responses.

Antibody-based IL-15 depletion or transfer of *IL-15R*-deficient T-cells caused loss of leukemia-control despite sorafenib-treatment (Fig.2d–f). The sorafenib/T-cell combination improved survival in three humanized AML models using human primary AML[FLT3-ITD] cells, MV4-11 (AML[FLT3-ITD]cell line) or MOLM-13 (AML[FLT3-ITD]cell line) cells (Fig.2g–i).

Donor CD8^{+} T-cells displayed higher expression of the anti-tumor cytotoxicity marker[15] CD107a, of IFN-γ, and CD40L in allo-HCT recipients that had received sorafenib compared to vehicle (Fig.3a–c, Suppl.Fig.2a,b). IL-15 increased the frequency of CD8^{+}CD107a^{+} T-cells *in vitro* compared to vehicle (Suppl.Fig.2c,d). IL-15R-activation leads to STAT5-phosphorylation[16] and higher phospho-STAT5-levels were found in CD8^{+} T-cells derived from sorafenib-treated mice (Fig.3d). Depletion of grafts for CD8^{+}T-cells but not for NK-cells (Suppl.Fig.2e) caused loss of the protective sorafenib-effect (Fig.3e) indicating that CD8^{+}T-cells mediate the sorafenib-induced anti-tumor effect.

To understand if recall-immunity developed under sorafenib-treatment, we next isolated CD8^{+}H-2Kb^{+}T-cells from mice that had received either Ba/F3-ITD-leukemia + T-cells + vehicle or Ba/F3-ITD-leukemia + T-cells + sorafenib (Suppl.Fig.2f). CD8^{+}H-2Kb^{+} T-cells isolated from allo-HCT recipients that had received Ba/F3-ITD-leukemia, T-cells and sorafenib but not the same cell population from mice treated with vehicle or sorafenib + anti-IL-15 caused long-term control of leukemia in secondary Ba/F3-ITD-leukemia cells-bearing mice (Fig.3f–h). Donor T-cells in sorafenib-treated recipients exhibited features of longevity[17,18] including high Bcl-2-expression and reduced PD-1-expression (Fig.3i,j).

Target-specificity of the recall-immune response was reflected by the fact that T-cells isolated from sorafenib-treated primary Ba/F3-ITD-leukemia-bearing recipients did not control third-party WEHI-3B-cells (Suppl.Fig.2g–i). IL-15 production upon sorafenib-exposure *in vitro* was not seen in FLT3-ITD-negative leukemia cell lines (Suppl.Fig.3a,b), and FLT3-ITD-negative WEHI-3B-cells could not induce recall-immunity (Suppl.Fig.3c,d).

The interferon-regulatory-factor-7 (IRF7) is an essential upstream activator of IL-15 transcription[19,20]. Activating transcription factor-4 (ATF4) blocks IRF7-phosphorylation and activation[21], thereby preventing IL-15 transcription. We observed reduced *Atf4* mRNA and protein in mouse and human FLT3-ITD-driven leukemia cells upon sorafenib-exposure (Fig. 4a,b, Suppl.Fig.4a–c), but not in sorafenib-resistant or FLT3-ITD[negative] leukemia cells (Suppl.Fig.4d–f). Consistent with decreased negative regulation by ATF4, the amount of active IRF7 (pIRF7/tIRF7) increased upon sorafenib-treatment in mouse and human

leukemia cells (Fig.4c–e, Suppl.Fig.4g) but not in sorafenib-resistant leukemia cells (Suppl.Fig.4h). Increased IL-15-production (Fig.4f), IRF7-activation (Suppl.Fig.4i,j), extended survival (Fig.4g), reduced leukemia cell counts in the peripheral blood (Suppl.Fig. 4k) upon sorafenib-treatment were abrogated by ATF4-overexpression (Suppl.Fig.4l). IRF7-knockdown (Suppl.Fig.4m) caused reduced levels of IL-15-production by human AML$^{FLT3-ITD}$-cells and loss of extended survival upon sorafenib-treatment (Fig.4h,i). Kinome analysis and subsequent kinase-inhibition of human AML$^{FLT3-ITD}$-cells revealed selectivity of sorafenib for IL-15 production (Suppl.Fig.5,6). Sorafenib binding-partner analysis identified no other kinases directly linked to IL-15-production (Suppl.Fig.7). Based on these observations, we propose a mechanism where sorafenib increases IL-15 production via inhibition of the negative regulatory-function of ATF4 in FLT3-ITD$^+$AML resulting in IRF7-activation (Fig.4j).

Comparable to sorafenib other FLT3-inhibitors increased IL-15 production (Suppl.Fig.8a–q). Consistent with our findings in mouse leukemia cells, we observed that *in vitro* sorafenib-exposure increased *IL-15* mRNA in primary human FLT3-ITD$^+$AML cells but not in FLT3-ITD^{negative}AML cells (Fig.5a–d).

Additionally, IL-15 serum levels, IL-15/pIRF7 protein in the BM and *IL-15* mRNA in leukemia cells increased in FLT3-ITD$^+$AML patients upon sorafenib-treatment (Fig.6a–c, Suppl.Fig.9a–c), and declined when the leukemia-burden was reduced (Suppl.Fig.9d). We analyzed separately responders (hematological complete-remission after sorafenib/DLI-treatment) and non-responders (no complete-remission). The IL-15/pIRF7-increase was not seen in non-responders (Fig.6a–c) and no increase was seen for other cytokines (Suppl.Fig. 9e–i). Increased IFN-γ serum levels (Fig.6d) and frequencies of IFN-γ$^+$CD8$^+$T-cells (Suppl.Fig.9j,k) were found in DLI/sorafenib-responders. Furthermore, Perforin$^+$CD8$^+$T-cells increased in DLI/sorafenib-responders, but not in non-responders (Suppl.Fig.9l,m).

Whole genome-sequencing of human primary FLT3-ITD$^+$AML cells indicated variable somatic mutation-frequencies and copy-number alterations, irrespective of the responder/non-responder group (Suppl.Fig.10a–c). FLT3-inhibitor-resistance mutations (D839G-FLT3, D835Y-FLT3[22]) were detected in several non-responders, but not in any of the responders (Suppl.Fig.10d). Annotating all mutations within a given distance around the transcription start site of the Interferon-regulatory-factor (*IRF*) genes according to the chromatin-state of monocytes, we found a reduction in the number of germline-mutations for Tx (strong transcription)- and TxW (weak transcription)-sites around *IRF7* in the AMLs of DLI/sorafenib-non-responders compared to DLI/sorafenib-responders (Fig.6e). *IL-15* mRNA-expression was upregulated after sorafenib-treatment only in responders (Suppl.Fig.11a).

Mitochondrial spare respiratory capacity (SRC) and glycolytic capacity (GC) have been linked to prolonged T-cell survival and enhanced ability to respond to antigen-challenge[23–25]. To understand if the patients' T-cell metabolisms were linked to sorafenib-responsiveness, we determined the metabolic profile of their CD8$^+$ T-cells by measuring the oxygen consumption rate (OCR) and the extracellular acidification rate (ECAR) at baseline and during a mitochondrial fitness test[23]. In DLI/sorafenib-responder patients both the GC and SRC were significantly enhanced following sorafenib treatment (Fig.6f,g, Suppl.Fig.

11b,c). In contrast, no changes in metabolic profile were observed in DLI/sorafenib-non-responders (Fig.6h.i, Suppl.Fig.11d,e).

Shannon diversity index (DI) of complementarity-determining-region-3 amino acid-sequences for TCR-α/TCR-β-chains was significantly higher in non-responders (Fig.6j). This was confirmed by the analysis of the variable gene-usage for both TCR chains (Suppl.Fig.12a,b). These observations are in line with previous studies showing that DLI-response is linked to low TCR-repertoire diversity[26,27].

A retrospective analysis of 409 patients with FLT3-ITD[+]AML-relapse after allo-HCT showed the dismal prognosis of these patients (Suppl.Fig.13a–f, Suppl. Table 1–11).

Discussion

Consistent with our data, others have shown that reduced IL-15 serum levels are associated with increased relapse-risk after allo-HCT in AML patients[28]. GVL-activity[29,30] as well as GVHD-severity[31–33] increased upon administration of IL-15 after mouse allo-HCT. To limit systemic toxicity of IL-15 we use sorafenib, which induces IL-15-production directly in the leukemia cell itself, thereby promoting a strong GVL-effect without significant GVHD-induction. Consistent with these findings, others have reported the production of IL-15 by acute leukemia cells[34,35], however no strategy has been found to date to directly increase IL-15 production in the malignant cells themselves. Our observation is clinically highly relevant, because the relapse rate in patients with *FLT3*-ITD[+]AML is 52% at 3 years after allo-HCT and the prognosis for these relapsed patients is poor[36]. We also extended the previous clinical observation of a synergistic effect for sorafenib and allo-HCT in FLT3-ITD[+]AML[5] by delineating the immunological mechanism behind this observation, thereby providing a scientific rationale for using sorafenib to treat FLT3-ITD[+]AML-relapse.

In agreement with our results, it was shown that patients receiving preemptive sorafenib-treatment had lower relapse-rates and improved survival compared to the control group[8–11]. Sorafenib-related IL-15-production increased the longevity-phenotype of donor CD8^{+} T-cells and their ability to induce recall-immunity. The increased glycolytic capacity and mitochondrial SRC of CD8^{+}T-cells from DLI/sorafenib-responders with higher IL-15 serum levels is consistent with previous reports in CD8^{+}T-cells that indicate IL-15 promotes mitochondrial biogenesis and contributes to enhanced glycolytic response following antigen-challenge[24].

Overall, we provide mouse and human data that support a novel concept for post-allo-HCT FLT3-ITD[+]AML-relapse-treatment using sorafenib + DLI. We show that FLT3-inhibition reduced ATF4 expression, allowing activation of the pIRF7/IL-15-axis in leukemia cells which in turn promotes immune-memory against tumor cells, leading to immune-mediated cure of AML[FLT3-ITD]-relapse. A prospective study is required to determine if the sorafenib + DLI combination is superior over other treatments.

Online Methods

Additional information can be found at the "Life Sciences Reporting Summary"

Human subjects

Human sample collection and analysis were approved by the Institutional Ethics Review Board of the Medical center, University of Freiburg, Germany (Protocol numbers: 10024/13, 26/11, 509/16 "Analysis of patients with FLT3-ITD mutated AML after allogeneic hematopoietic cell transplantation") and the study was registered at ClinicalTrials.gov (number: NCT02867891). Written informed consent was obtained from each patient. All analysis of human data were carried out in compliance with relevant ethical regulations.

With IRB approval, we conducted a multicenter, retrospective analysis of FLT3-ITD+ AML patients who received any kind of therapy for hematological relapse after allo-HCT. We contacted transplant programs with the highest volumes of AML patients undergoing allo-HCT, as provided by the European Group for Blood and Marrow Transplantation (EBMT). Additional sites in the US, Canada, Japan and Australia were surveyed based on recommendation from these initial sites.

All data reported by the Transplant Centers is shown in Suppl. Table 1. Of 419 patients with FLT3-ITD+AML-relapse after allo-HCT 10 patients had to be excluded because they received no relapse treatment (n=6), had no hematological relapse (n=1), survival data was incomplete (n=1), time until second allo-HCT was unknown (n=1) and patient never being in remission after allo-HCT (n=1). All excluded patients are displayed in Suppl. Table 1. The resulting 409 patients with FLT3-ITD+AML-relapse after allo-HCT were analyzed for response rates and OS.

The decision on the treatment of relapse was made by the individual centers and based on published literature providing a scientific rationale for DLI[38–40] and DLI combined with sorafenib [5]. To date, no international guidelines or clinical pathway recommendations exist specifically for patients relapsing with FLT3-ITD+ AML after allo-HCT. Sorafenib was given at a dosage of 400 mg twice daily.

The patients' characteristics, including recipient age and gender, AML characteristics, donor type, conditioning regimen, immunosuppressive regimen and remission status before transplant are detailed in Suppl. Table 1 for each individual patient. The data for each treatment group are summarized in Suppl. Tables 2–11.

Mice

C57BL/6 (H-2Kb, Thy-1.2), BALB/c (H-2Kd, Thy-1.2), NSG mice and $Rag2^{-/-}Il2r\gamma^{-/-}$ mice were purchased either from Charles River Laboratory (Sulzfeld, Germany), Janvier Labs (France) or from the local stock of the animal facility at University of Freiburg. $Il\text{-}15^{-/-}$ mice were provided by Dr. Y. Tanriver (University of Freiburg). $Il\text{-}15Ra^{-/-}$ mice were provided by Dr. B. Becher (University of Zurich). Mice were used between 6 and 12 weeks of age and only female or male donor/recipient pairs were used. Animal experiments were carried out in compliance with relevant animal use guidelines and ethical regulations Animal protocols (Protocol numbers: G13-116, G-15/018, G-16/018, G-17/093) were approved by the Regierungspräsidium Freiburg, Freiburg, Germany (Federal Ministry for Nature, Environment and Consumers' Protection).

Immunologic analysis

Correlative studies were performed at baseline and on different days after the start of sorafenib treatment, as indicated in the individual figure legends. These studies included the following: immunophenotypic analysis of peripheral-blood mononuclear cells by means of flow cytometry; immunohistochemical staining of formalin-fixed, paraffin-embedded BM biopsy specimens, whole exome sequencing of enriched AML cells, DNA sequencing of the TCR chains of enriched T-cells, analysis of CD8^{+} T-cell metabolism, microarray of enriched AML cells and cytokine/chemokine assays of plasma samples.

Metabolism assays (sea-horse) of human CD8+ T-cells

Oxygen consumption rates (OCR) and extracellular acidification rates (ECAR) of human CD8^{+} T-cells were measured in XF media (non-buffered RPMI 1640 containing 25 mM glucose, 2 mM L-glutamine, and 1 mM sodium pyruvate) under basal conditions and in response to 1 μM oligomycin, 1.5 μM fluoro-carbonyl cyanide phenylhydrazone (FCCP) and 100 nM rotenone + 1 μM antimycin A, (all Sigma) using a 96-well XFe Extracellular Flux Analyzer (Seahorse Bioscience) as previously described[41].

Whole Genome Sequencing

Whole Genome Sequencing was performed on 4 tumor samples on Illumina HiSeq X. Each sample was sequenced on 4 lanes to insure a good coverage. After bad quality read trimming[42], reads were aligned on Human reference genome hg19 using BWA aligner[43]. Duplicate-removal, indel realignment and base quality recalibration were performed using Genome Analysis Toolkit[44]. We called SNP and Indel mutations and applied false positive filtering using Varscan2. Relevant mutations were selected as follows: Read depth > 8 reads per base, variant allele frequency > 9%, MAF from Exome Aggregation Consortium[45](ExAC) < 0.1%. Copy number alteration analysis was achieved using Control-FREEC[46].

Gene expression analysis of responder and non-responder patients after sorafenib treatment

RNA from PBMC of 8 patients at 2 different time points (3 days before and 6 days after Sorafenib treatment) were extracted from 8 ml of blood. 2 ug of total RNA from around 10^7 cells per sample were incubated with DNaseI according to the manufacturer's instruction (Qiagen, Germany) and cleaned up with RNeasy Micro Kit (Qiagen, Germany). RNA integrity was analyzed by capillary electrophoresis using a Fragment Analyser (Advanced Analytical Technologies, Inc. Ames, IA). RNA samples were further processed with the Affymetrix GeneChip Pico kit and hybridized to Affymetrix Clariom S arrays as described by the manufacturer (Affymetrix, USA). The arrays were normalized via robust multichip averaging as implemented in the R/Bioconductor oligo package[47]. Gene set enrichment was calculated using the R/Bioconductor package 'gage'[48] using the pathways from the ConsensusPathDB [49] as gene sets and a significance cutoff p<0.05.

The data is available to the reviewers following the private link https://www.ncbi.nlm.nih.gov/geo/query/acc.cgi?token=ufmxwqyeplyxlon&acc=GSE95770 (GEO accession number: GSE95770).

Overexpression of ATF4 in Ba/F3-ITD cells

The lentiviral vector overexpressing mouse ATF4, mATF4 (Plasmid #24874) was purchased from Addgene, USA. The packaging cell line, 293T was purchased from Clontech, France and was cultured in DMEM, high glucose, GlutaMAX Supplement, pyruvate (Gibco, Germany) supplemented with 10% FCS (PAN-Biotech, Germany) and 1% Pencillin/ Streptomycin (Gibco, Germany). The packaging cells were transiently transfected with 10 μg of mATF4 and 10 μg of envelope vector pVSV-G using $CaCl_2$, and the viral stocks were collected after 48 and 72 hours following transfection. We used these viral stocks to transduce Ba/F3-ITD cells and the cells were cultured in 2 μg/ml Puromycin (Invivogen, France) for the selection of transduced cells. The overexpression of ATF4 in the Puromycin-selected cells was further confirmed by Western blotting.

Knockdown of IRF7 in MOLM-13 cells

HEK293T packaging cells were cultured as described previously[50]. The doxycycline inducible lentiviral vectors, pTRIPZ inducible lentiviral human IRF7 shRNA (Clone ID:V3THS_356931) and TRIPZ Inducible Lentiviral Non-silencing (NS) shRNA Control (#RHS4743) with turboRFP reporter were purchased from Dharmacon, Germany. The lentiviral particles were generated by transfection of HEK293T-cells using Polyethylenimine (Polysciences) and the Trans-Lentiviral Packaging System (Dharmacon, Germany). 5×10^5 MOLM-13 cells were transduced with the lentiviral particles (transfected cells annotated as MOLM-13[NS shRNA] and MOLM-13[IRF7 shRNA]). The cells were selected in 2 μg/ml Puromycin (Invivogen, Germany) 24 hours post infection. The cells were cultured in media containing 2 μg/ml doxycycline for 11 days for the expression of inducible shRNA. The knockdown of IRF7 was confirmed by Western blotting.

Bone marrow (BM) transplantation model and histopathology scoring

BM transplantation experiments were performed as previously described[51,52]. Briefly, recipients were injected intravenously (i.v.) with 5×10^6 WT BM cells after lethal irradiation with 9–11 Gy. To induce GvHD, $CD4^+$ and $CD8^+$ T-cells were isolated from donor spleens and enriched by positive selection with the MACS cell separation system (Miltenyi Biotec, USA) according to the manufacturer's instructions. Anti-CD4 and anti-CD8 MicroBeads were used. $CD4^+/CD8^+$ T-cell purity was at least 90% as assessed by flow cytometry (data not shown). $CD4^+/CD8^+$ T-cells were given at a dosage of 2×10^5 (C57BL/6-derived) or 5×10^5 (BALB/c-derived) i.v. on day 2 following the transplantation of BM cells with or without leukemia cells. Slides of small intestine, large intestine, and liver specimens collected after allo-HCT were stained with Hematoxylin/Eosin and scored by an experienced pathologist blinded to the treatment groups. GVHD severity was determined according to a previously published histopathology scoring system[53].

Depletion of NK cells

To deplete NK cells, BM was stained for CD3 and NK1.1 surface markers. BM was depleted of $NK1.1^+CD3^-$ cells using FACS sorting by excluding all $NK1.1^+CD3^-$ cells.

Quantitative PCR (qPCR) for IL-15 expression from murine and human cells

Murine Ba/F3-ITD cells were treated with DMSO or different concentrations of sorafenib, tandutinib, crenolanib, midostaurin or quizartinib for 24 hours as indicated in the individual figure legends. Total RNA was isolated using miRNeasy Mini kit (Qiagen, Netherlands) or isolated using Qiazol lysis reagent (Qiagen, Netherlands) according to manufacturer's instructions. 1 μg of total RNA from treated Ba/F3-ITD cells was reverse transcribed into complementary DNA (cDNA) using the High-Capacity cDNA Reverse Transcription Kit (ThermoScientific, USA). Quantitive PCR (qPCR) was carried out using the LightCycler® 480 SYBR Green I Master kit (Roche, Switzerland) in a LightCyler 480 (Roche, Switzerland). 50–80 ng cDNA was used for qPCR analysis. For analysis of mouse *Il-15* mRNA expression from Ba/F3-ITD cells, primers (sense primer: 5′-CATCCATCTCGTGCTACTT-3′, anti-sense primer: 5′-TTCTCCAGGTCATATCTTACAT-3′) were designed using Beacon Designer software (Premier Biosoft, UK) and were synthesized by Apara Biosciences, Germany. Reference gene was selected using the Primer only geNorm 12 gene kit for use with SYBR green (ge-SY-12, PrimerDesign, UK) and geNorm analysis software (PrimerDesign, USA) according to the manufacturer's instruction. *Mon2* was used as the reference gene to which the *Il-15* mRNA expression was normalized. Mouse *Il-15* primers were synthesized and purchased from Apara Biosciences, Germany whereas *Mon2* primers were purchased from PrimerDesign, USA.

For analysis of human *IL-15* mRNA expression, MV-411 cells, MOLM-13[NS shRNA] cells, MOLM-13[NS shIRF7] cells, HL60, NB4 and U937 and human PBMC were treated with DMSO or different concentrations of sorafenib, quizartinib or tandutinib for 24 hours or 48 hours as indicated in the figure legends. Cells were harvested and lysed in Qiazol lysis reagent (Qiagen, Netherlands) and total RNA was isolated according to manufacturer's instructions. 300ng–1μg of total RNA was reverse transcribed into complementary DNA (cDNA) using the High-Capacity cDNA Reverse Transcription Kit (ThermoScientific, USA). QPCR was carried out using the LightCycler® 480 SYBR Green I Master kit (Roche, Switzerland) in a LightCyler 480 (Roche, Switzerland). 50 ng cDNA was used for qPCR analysis. RT^2 qPCR Primer Assay for Human IL15 (QIAGEN, Netherlands) was used for detecting human *IL-15* mRNA expression. Reference gene was selected using the Primer only geNorm 12 gene kit for use with SYBR green (ge-SY-12, PrimerDesign, UK) and geNorm analysis software (PrimerDesign, USA) according to the manufacturer's instruction. *GAPDH* was used as the reference gene (sense primer: 5′-CTCCTCCACCTTTGACGCTG-3′, anti-sense primer: 5′-ACCACCCTGTTGCTGTAGCC-3′) for untreated human PBMC or human PBMC treated with DMSO or Sorafenib and for MV4-11 cells treated with DMSO or different concentrations of tandutinib or quizartinib. Human *GAPDH* primers were synthesized and purchased from Apara Bioscience, Germany or Eurofins Genomics, Germany. *ENOX-2* was used as the reference gene for MOLM-13[NS shRNA] cells and MOLM-13[NS shIRF7] cells which were treated with DMSO or different concentrations of Sorafenib. *ENOX-2* primers were purchased from PrimerDesign, USA.

Flow cytometry

All antibodies used for flow cytometry are listed in Suppl. Table 12. For all fluorochrome-conjugated antibodies, optimal concentrations were determined using titration experiments. Cells were incubated with the respective antibodies diluted in FACS buffer for 20 minutes at 4°C for surface antigen staining. Cells were then washed with FACS buffer according to the manufacturer's instruction For murine pSTAT5 expression analysis, cells were fixed with one part pre-warmed 3.7% formalin and one part FACS buffer; and then exposed to 90% methanol, before application of the pSTAT5 antibody. All intracellular cytokine stainings were performed using BD Cytofix/Cytoperm kit (BD Biosciences, Germany). For intracellular cytokine staining for murine IFN-γ, cells were restimulated with 0.5 μg/ml Phorbol 12-Myristate 13 Acetate (Sigma-Aldrich, Germany) and 50ng/ml Ionomycin (Sigma-Aldrich, Germany) for 5 hours, and 1 μl/ml media of Brefeldin A (Golgi Plug, BD Biosciences, Germany) was added at the end of 2 hours prior to staining. For intracellular staining of IL-15, cells were treated with 1 μl/ml media of Brefeldin A (Golgi Plug, BD Biosciences, Germany) for 8 hours prior to staining with unconjugated anti-IL-15 (overnight staining at 4°C). The cells were then stained with secondary antibody F(ab′)2 Anti-Rat IgG APC (eBioscience, Germany). For intracellular staining of human IFN-γ and Perforin, cells were fixed with 4% Paraformaldehyde and stained in 1X BD Perm/Wash Buffer according to manufacturer's instruction. For excluding dead cells, the live/dead fixable dead cell stain kit from Molecular Probes, USA was used according to the manufacturer's instructions. Data was acquired on the BD LSR Fortessa (BD Biosciences, Germany) or Flow Cytometer CyAn[TM] ADP (Beckman Coulter, Germany) and analyzed using Flow Jo software (Tree Star, USA). The gating strategy is provided in Suppl. Figure 14.

Statistical analysis

For the sample size in the murine GvL survival experiments a power analysis was performed. A sample size of at least n= 8 per group was determined by 80% power to reach a statistical significance of 0.05 to detect an effect size of at least 1.06. For the xenograft model, n=7 per group was used because of the higher difference expected in this experimental setting. Differences in animal survival (Kaplan-Meier survival curves) were analyzed by Mantel Cox test. The experiments were performed in a non-blinded fashion except for the GVHD severity scoring. To obtain unbiased data, the histopathological scoring of GvHD severity was performed by a pathologist blinded to both the genotype and the treatment group. Only after finalization of the quantitative GvHD severity scores the samples were allocated to their genotypes/treatment group. There was no randomization of mice or samples before analysis. All samples or mice were included in our analysis.

For statistical analysis an unpaired *t*-test (two-sided) was applied. All data were tested for normality applying the Kolmogorov-Smirnov test. If the data did not meet the criteria of normality, the Mann-Whitney *U* test was applied. Wilcoxon matched-pairs signed rank test was used to analyze related samples. Data are presented as mean and s.e.m. (error bars). Differences were considered significant when the *P*-value was <0.05.

Patient data were analyzed using SAS 9.2 (SAS Institute Inc., Cary, NC, USA). OS was calculated as the time from start of treatment until the date of death from any cause. Patients

alive at the end of the observation period were censored at the time last seen alive. OS rates and median survival times were estimated using the Kaplan-Meier method.

Supplementary Material

Refer to Web version on PubMed Central for supplementary material.

Authors

Nimitha R. Mathew[1,2], Francis Baumgartner[1], Lukas Braun[1], David O'Sullivan[3], Simone Thomas[4], Miguel Waterhouse[1], Tony A. Müller[1], Kathrin Hanke[1,2], Sanaz Taromi[1], Petya Apostolova[1], Anna L. Illert[1], Wolfgang Melchinger[1], Sandra Duquesne[1], Annette Schmitt-Graeff[5], Lena Osswald[1], Kai-Li Yan[1], Arnim Weber[6], Sonia Tugues[7], Sabine Spath[7], Dietmar Pfeifer[1], Marie Follo[1], Rainer Claus[1], Michael Lübbert[1], Christoph Rummelt[1], Hartmut Bertz[1], Ralph Wäsch[1], Johanna Haag[1], Andrea Schmidts[1], Michael Schultheiss[8], Dominik Bettinger[8], Robert Thimme[8], Evelyn Ullrich[9], Yakup Tanriver[6,10], Giang Lam Vuong[11], Renate Arnold[11], Philipp Hemmati[11], Dominik Wolf[12], Markus Ditschkowski[13], Cordula Jilg[14], Konrad Wilhelm[14], Christian Leiber[14], Sabine Gerull[15], Jörg Halter[15], Claudia Lengerke[15], Thomas Pabst[16], Thomas Schroeder[17], Guido Kobbe[17], Wolf Rösler[18], Soroush Doostkam[19], Stephan Meckel[20], Kathleen Stabla[21], Stephan K. Metzelder[21], Sebastian Halbach[22], Tilman Brummer[22,23,24], Zehan Hu[25], Joern Dengjel[25], Björn Hackanson[26], Christoph Schmid[26], Udo Holtick[27], Christof Scheid[27], Alexandros Spyridonidis[28], Friedrich Stölzel[29], Rainer Ordemann[29], Lutz P. Müller[30], Flore Sicre-de-Fontbrune[31], Gabriele Ihorst[32], Jürgen Kuball[33], Jan E. Ehlert[34], Daniel Feger[34], Eva-Maria Wagner[35], Jean-Yves Cahn[36], Jacqueline Schnell[37], Florian Kuchenbauer[37], Donald Bunjes[37], Ronjon Chakraverty[38], Simon Richardson[38], Saar Gill[39], Nicolaus Kröger[40], Francis Ayuk[40], Luca Vago[41], Fabio Ciceri[41], Antonia M. Müller[42], Takeshi Kondo[43], Takanori Teshima[43], Susan Klaeger[23,44], Bernhard Kuster[44], Dennis (Dong Hwan) Kim[45], Daniel Weisdorf[46], Walter van der Velden[47], Daniela Dörfel[48], Wolfgang Bethge[48], Inken Hilgendorf[49], Andreas Hochhaus[49], Geoffroy Andrieux[50], Melanie Börries[50], Hauke Busch[50,51], John Magenau[52], Pavan Reddy[52], Myriam Labopin[53], Joseph H. Antin[54], Andrea S. Henden[55], Geoffrey R. Hill[55,56], Glen A. Kennedy[56], Merav Bar[57], Anita Sarma[58], Donal McLornan[58], Ghulam Mufti[58], Betul Oran[59], Katayoun Rezvani[59], Omid Sha[60], Robert S. Negrin[60], Arnon Nagler[61], Marco Prinz[20,24], Andreas Burchert[22], Andreas Neubauer[22], Dietrich Beelen[14], Andreas Mackensen[19], Nikolas von Bubnoff[1], Wolfgang Herr[4], Burkhard Becher[7], Gerard Socié[31], Michael A. Caligiuri[62], Eliana Ruggiero[41], Chiara Bonini[41], Georg Häcker[6], Justus Duyster[1], Jürgen Finke[1], Erika Pearce[3], Bruce R. Blazar[63], and Robert Zeiser[1,24]

Affiliations

[1]Department of Hematology, Oncology and Stem Cell Transplantation, Medical Center - University of Freiburg, Faculty of Medicine, University of Freiburg, Freiburg, Germany [2]Faculty of Biology, Albert-Ludwigs-University, Freiburg, Germany [3]Max Planck Institute for Immunobiology and Epigenetics, Freiburg, Germany

[4]Department of Internal Medicine III, Hematology and Oncology, University Hospital Regensburg, Germany [5]Department of Pathology, University Medical Center Freiburg, Freiburg, Germany [6]Department of Medical Microbiology and Hygiene, University Medical Center Freiburg, Freiburg, Germany [7]Institute of Experimental Immunology, University of Zurich, Zurich, Switzerland [8]Department of Medicine II, Medical Center University of Freiburg, Faculty of Medicine, University of Freiburg, Hugstetter Str. 55, D-79106 Freiburg, Germany [9]University Hospital Frankfurt, Department for Children and Adolescents Medicine, Division of Stem Cell Transplantation and Immunology, Goethe-University, Frankfurt, Germany [10]Department of Nephrology, University Medical Center Freiburg, Freiburg, Germany [11]Department of Stem Cell Transplantation, Charité University Medicine Berlin, Germany [12]Medical Clinic III, Oncology, Hematology, Immunooncology and Rheumatology, University Hospital Bonn (UKB), Bonn, Germany [13]Department of Bone Marrow Transplantation, West German Cancer Center, University Hospital Essen, Germany [14]Department of Urology, University Medical Center Freiburg, Freiburg, Germany [15]Division of Hematology, University Hospital Basel, Basel, Switzerland [16]Inselspital/Universitätsspital Bern, CH-3010 Bern, Switzerland [17]Department of Hematology, Oncology and Clinical Immunology, Universitätsklinikum Düsseldorf, Düsseldorf, Germany [18]Department of Hematology and Oncology, University of Erlangen, Germany [19]Institute for Neuropathology, University of Freiburg, Germany [20]Department of Neuroradiology, University Medical Center Freiburg, Freiburg, Germany [21]Department of Hematology, Oncology and Immunology, Philipps University Marburg, and University Medical Center Giessen and Marburg, Marburg, Germany [22]Institute of Molecular Medicine and Cell Research (IMMZ), Faculty of Medicine, Albert-Ludwigs-University Freiburg, Germany [23]German Cancer Consortium (DKTK), partner site Freiburg; and German Cancer Research Center (DKFZ), Heidelberg, Germany, Freiburg, Germany [24]Center for Biological signaling studies (BIOSS) - University of Freiburg, Germany [25]Department of Dermatology, Medical Center - University of Freiburg, Germany; and Department of Biology, University of Fribourg, Fribourg, Switzerland [26]Interdisziplinäres Cancer Center Augsburg (ICCA), II. Medizinische Klinik, Augsburg, Germany [27]Department of Internal Medicine I, University Hospital Cologne, Germany [28]Hematology Stem cell transplant Unit, Patras, Greece [29]Department of Hematology and Oncology, Universitätsklinikum Carl Gustav Carus an der Technischen Universität Dresden, Germany [30]Department of Hematology and Oncology, Universitätsklinikum Halle, Halle, Germany [31]APHP, Saint Louis Hospital, Hematology Stem cell transplantation, & Inserm UMR 1160, Paris, France [32]Clinical Trials Unit, Faculty of Medicine and Medical Center - University of Freiburg, Germany [33]Department of Hematology, University Medical Center Utrecht, The Netherlands [34]ProQinase GmbH, Freiburg, Germany, Freiburg [35]Dept. of Hematology and Oncology, Universitaetsmedizin Mainz, Mainz, Germany [36]Clinique Universitaire Hématologie, Université Grenoble Alpes, France [37]Department of Internal Medicine III, University Hospital of Ulm, Ulm, Germany [38]Cancer Institute and Institute of Immunity and Transplantation, Royal Free Hospital, London, UK

[39]Hospital of the University of Pennsylvania, Smilow Translational Research Center, Philadelphia, PA, USA [40]Department of Stem Cell Transplantation, University Hospital Hamburg-Eppendorf, Germany [41]Unit of Immunogenetics, Leukemia Genomics and Immunobiology, Unit of Hematology and Bone Marrow Transplantation, San Raffaele Scientific Institute, and University Vita-Salute San Raffaele Milano, Italy [42]Department of Hematology, University Hospital Zurich, Zurich, Switzerland [43]Department of Hematology, Hokkaido University, Sapporo, Japan [44]Proteomics and Bioanalytics, Technische Universitaet Muenchen, Partner Site of the German Cancer Consortium, Freising, Germany [45]Department of Medical Oncology & Hematology, Princess Margaret Cancer Centre, University of Toronto, Ontario, Canada [46]Hematology, Oncology and Transplantation University of Minnesota, Minneapolis, USA [47]Department of Hematology, Radboud University, Nijmegen, Netherlands [48]Medizinische Klinik II, Universitätsklinikum Tübingen, Tübingen, Germany [49]Klinik für Innere Medizin II, Universitätsklinikum Jena, Jena, Germany [50]Systems Biology of the Cellular Microenvironment Group, IMMZ, ALU, Freiburg, Germany. German Cancer Consortium (DKTK), Freiburg, Germany. German Cancer Research Center (DKFZ), Heidelberg, Germany [51]Institute of Experimental Dermatology, University of Lübeck, Lübeck, Germany [52]Department of Hematology, University of Michigan Medical School, Ann Arbor, Michigan, USA [53]EBMT Statistical Unit, Hôpital Saint Antoine Paris, France [54]Dana-Farber Cancer Institute, Harvard Medical School, Boston, MA, USA [55]Bone Marrow Transplant Laboratory, QIMR Berghofer Medical Research Institute, Brisbane, Australia & Department of Haematology, Royal Brisbane Hospital, Brisbane, Australia [56]Department of Haematology, Royal Brisbane and Womens Hospital, Brisbane, Australia [57]Division of Blood and Marrow Transplantation, Fred Hutchinson Cancer Research Center, University of WA Seattle, USA [58]Department of Haematological Medicine, King's College Hospital NHS Foundation Trust, London, UK [59]Division of BMT, MD Anderson Cancer Center, Houston, TX, USA [60]Division of Blood and Marrow Transplantation, Stanford University Medical School, Stanford, CA, USA [61]Division of Hematology, Chaim Sheba Medical Center, Tel Hashomer, Israel [62]The Ohio State University Comprehensive Cancer Center, Columbus, USA [63]Department of Pediatrics, Division of Blood and Marrow Transplantation, University of Minnesota, Minneapolis, Minnesota, USA

Acknowledgments

References

1. Pfirrmann M, Ehninger G, Thiede C, Bornhäuser M, Kramer M, Röllig C, Hasford J, Schaich M. Prediction of post-remission survival in acute myeloid leukaemia: a post-hoc analysis of the AML96 trial. Lancet Oncol. 2012; 13:207–214. [PubMed: 22197676]

2. Sengsayadeth SM, Jagasia M, Engelhardt BG, et al. Allo-SCT for high-risk AML-CR1 in the molecular era: impact of FLT3/ITD outweighs the conventional markers. Bone Marrow Transplant. 2012; 47:1535–1537. [PubMed: 22659680]

3. Serve H, Krug U, Wagner R, Sauerland MC, Heinecke A, Brunnberg U, et al. Sorafenib in combination with intensive chemotherapy in elderly patients with acute myeloid leukemia: results from a randomized, placebo-controlled trial. J Clin Oncol. 2013; 31:3110–3118. [PubMed: 23897964]

4. Röllig C, Serve H, Hüttmann A, Noppeney R, Müller-Tidow C, Krug U, et al. Addition of sorafenib versus placebo to standard therapy in patients aged 60 years or younger with newly diagnosed acute myeloid leukaemia (SORAML): a multicentre, phase 2, randomised controlled trial. Lancet Oncol. 2015:1691–1699. [PubMed: 26549589]

5. Metzelder SK, Schroeder T, Finck A, Scholl S, Fey M, Götze K, et al. High activity of sorafenib in FLT3-ITD-positive acute myeloid leukemia synergizes with allo-immune effects to induce sustained responses. Leukemia. 2012; 26:2353–2359. [PubMed: 22504140]

6. Tschan-Plessl A, Halter JP, Heim D, Medinger M, Passweg JR, Gerull S. Synergistic effect of sorafenib and cGvHD in patients with high-risk FLT3-ITD+AML allows long-term disease control after allogeneic transplantation. Ann Hematol. 2015; 94:1899–1905. [PubMed: 26233683]

7. Krüger WH, Hirt C, Kiefer T, Neumann T, Busemann C, Dölken G. Molecular remission of FLT3-ITD (+) positive AML relapse after allo-SCT by acute GVHD in addition to sorafenib. Bone Marrow Transplant. 2012; 47:137–138. [PubMed: 21423122]

8. Chen YB, Li S, Lane AA, Connolly C, Del Rio C, Valles B, Curtis M, Ballen K, Cutler C, Dey BR, El-Jawahri A, Fathi AT, Ho VT, Joyce A, McAfee S, Rudek M, Rajkhowa T, Verselis S, Antin JH, Spitzer TR, Levis M, Soiffer R. Phase I trial of maintenance sorafenib after allogeneic hematopoietic stem cell transplantation for fms-like tyrosine kinase 3 internal tandem duplication acute myeloid leukemia. Biol Blood Marrow Transplant. 2014; 20:2042–2048. [PubMed: 25239228]

9. Antar A, Kharfan-Dabaja MA, Mahfouz R, Bazarbachi A. Sorafenib Maintenance Appears Safe and Improves Clinical Outcomes in FLT3-ITD Acute Myeloid Leukemia After Allogeneic Hematopoietic Cell Transplantation. Clin Lymphoma Myeloma Leuk. 2015; 15:298–302. [PubMed: 25550214]

10. Tarlock K, Chang B, Cooper T, Gross T, Gupta S, Neudorf S, Adlard K, Ho PA, McGoldrick S, Watt T, Templeman T, Sisler I, Garee A, Thomson B, Woolfrey A, Estey E, Meshinchi S, Pollard JA. Sorafenib treatment following hematopoietic stem cell transplant in pediatric FLT3/ITD acute myeloid leukemia. Pediatr Blood Cancer. 2015; 62:1048–1054. [PubMed: 25662999]

11. Brunner AM, Li S, Fathi AT, Wadleigh M, Ho VT, Collier K, Connolly C, Ballen KK, Cutler CS, Dey BR, El-Jawahri A, Nikiforow S, McAfee SL, Koreth J, Deangelo DJ, Alyea EP, Antin JH, Spitzer TR, Stone RM, Soiffer RJ, Chen YB. Haematopoietic cell transplantation and with without sorafenib maintenance for patients with FLT3-ITD acute myeloid leukaemia in first complete remission. Br J Haematol. 2016; 175:496–504. [PubMed: 27434660]

12. Zorko NA, Bernot KM, Whitman SP, Siebenaler RF, Ahmed EH, Marcucci GG, Yanes DA, McConnell KK, Mao C, Kalu C, Zhang X, Jarjoura D, Dorrance AM, Heerema NA, Lee BH, Huang G, Marcucci G, Caligiuri MA. Mll partial tandem duplication and Flt3 internal tandem duplication in a double knock-in mouse recapitulates features of counterpart human acute myeloid leukemias. Blood. 2012; 120:1130–1136. [PubMed: 22674806]

13. Bernot KM, Nemer JS, Santhanam R, Liu S, Zorko NA, Whitman SP, et al. Eradicating acute myeloid leukemia in a Mll(PTD/wt):Flt3(ITD/wt) murine model: a path to novel therapeutic approaches for human disease. Blood. 2013; 122:3778–3783. [PubMed: 24085765]

14. Lucas M, Schachterle W, Oberle K, Aichele P, Diefenbach A. Dendritic cells prime natural killer cells by trans-presenting interleukin 15. Immunity. 2007; 26:503–517. [PubMed: 17398124]

15. Rubio V, Stuge TB, Singh N, Betts MR, Weber JS, Roederer M, Lee PP. Ex vivo identification, isolation and analysis of tumor-cytolytic T cells. Nature medicine. 2003; 9:1377–1382.

16. Pandiyan P, Yang XP, Saravanamuthu SS, Zheng L, Ishihara S, O'Shea JJ, Lenardo MJ. The role of IL-15 in activating STAT5 and fine-tuning IL-17A production in CD4 T lymphocytes. J Immunol. 2012; 189:4237–4246. [PubMed: 22993203]

17. Patsoukis N, Bardhan K, Chatterjee P, Sari D, Liu B, Bell LN, Karoly ED, Freeman GJ, Petkova V, Seth P, Li L, Boussiotis VA. PD-1 alters T-cell metabolic reprogramming by inhibiting glycolysis and promoting lipolysis and fatty acid oxidation. Nat Commun. 2015; 6:6692–6697. [PubMed: 25809635]

18. van Bockel DJ, Price DA, Munier ML, Venturi V, Asher TE, Ladell K, Greenaway HY, Zaunders J, Douek DC, Cooper DA, Davenport MP, Kelleher AD. Persistent survival of prevalent clonotypes within an immunodominant HIV gag-specific CD8+ T cell response. J Immunol. 2011; 186:359–371. [PubMed: 21135165]

19. Azimi N, Shiramizu KM, Tagaya Y, Mariner J, Waldmann TA. Viral activation of interleukin-15 (IL-15): characterization of a virus-inducible element in the IL-15 promoter region. J Virol. 2000; 74:7338–7348. [PubMed: 10906187]

20. Romieu-Mourez R, Solis M, Nardin A, Goubau D, Baron-Bodo V, Lin R, Massie B, Salcedo M, Hiscott J. Distinct roles for IFN regulatory factor (IRF)-3 and IRF-7 in the activation of antitumor properties of human macrophages. Cancer Res. 2006; 66:10576–10585. [PubMed: 17079482]

21. Liang Q, Deng H, Sun CW, Townes TM, Zhu F. Negative regulation of IRF7 activation by activating transcription factor 4 suggests a cross-regulation between the IFN responses and the cellular integrated stress responses. J Immunol. 2011; 186:1001–1010. [PubMed: 21148039]

22. Smith CC, Lin K, Stecula A, Sali A, Shah NP. FLT3 D835 mutations confer differential resistance to type II FLT3 inhibitors. Leukemia. 2015; 29:2390–2392. [PubMed: 26108694]

23. Buck MD, O'Sullivan D, Pearce EL. T cell metabolism drives immunity. J Exp Med. 2015; 212:1345–1360. [PubMed: 26261266]

24. van der Windt GJ, Everts B, Chang CH, Curtis JD, Freitas TC, Amiel E, Pearce EJ, Pearce EL. Mitochondrial respiratory capacity is a critical regulator of CD8+ T cell memory development. Immunity. 2012; 36:68–78. [PubMed: 22206904]

25. van der Windt GJ, O'Sullivan D, Everts B, Huang SC, Buck MD, Curtis JD, Chang CH, Smith AM, Ai T, Faubert B, Jones RG, Pearce EJ, Pearce EL. CD8 memory T cells have a bioenergetic advantage that underlies their rapid recall ability. Proc Natl Acad Sci U S A. 2013; 110:14336–14341. [PubMed: 23940348]

26. Schultze-Florey C, Raha S, Ravens S, et al. TCR Diversity Is a Predictive Marker for Donor Lymphocyte Infusion Response. Blood. 2016; 128:4605.

27. van Bergen CA, van Luxemburg-Heijs SA, de Wreede LC, Eefting M, von dem Borne PA, van Balen P, Heemskerk MH, Mulder A, Claas FH, Navarrete MA, Honders WM, Rutten CE, Veelken H, Jedema I, Halkes CJ, Griffioen M, Falkenburg JH. Selective graft-versus-leukemia depends on magnitude diversity of the alloreactive T cell response. The Journal of clinical investigation. 2017; 127:517–529. [PubMed: 28067665]

28. Thiant S, Yakoub-Agha I, Magro L, Trauet J, Coiteux V, Jouet JP, Dessaint JP, Labalette M. Plasma levels of IL-7 and IL-15 in the first month after myeloablative BMT are predictive biomarkers of both acute GVHD and relapse. Bone Marrow Transplant. 2010; 45:1546–1552. [PubMed: 20190846]

29. Sauter CT, Bailey CP, Panis MM, Biswas CS, Budak-Alpdogan T, Durham A, Flomenberg N, Alpdogan O. Interleukin-15 administration increases graft-versus-tumor activity in recipients of haploidentical hematopoietic SCT. Bone Marrow Transplant. 2013; 48:1237–1242. [PubMed: 23624821]

30. Chen G, Wu D, Wang Y, Cen J, Feng Y, Sun A, Tang X, Chang H, Zhu Z. Expanded donor natural killer cell and IL-2, IL-15 treatment efficacy in allogeneic hematopoietic stem cell transplantation. Eur J Haematol. 2008; 81:226–235. [PubMed: 18573173]

31. Blaser BW, Roychowdhury S, Kim DJ, Schwind NR, Bhatt D, Yuan W, Kusewitt DF, Ferketich AK, Caligiuri MA, Guimond M. Donor-derived IL-15 is critical for acute allogeneic graft-versus-host disease. Blood. 2005; 105:894–901. [PubMed: 15374888]

Author Manuscript
Author Manuscript
Author Manuscript
Author Manuscript

32. Blaser BW, Schwind NR, Karol S, Chang D, Shin S, Roychowdhury S, Becknell B, Ferketich AK, Kusewitt DF, Blazar BR, Caligiuri MA. Trans-presentation of donor-derived interleukin 15 is necessary for the rapid onset of acute graft-versus-host disease but not for graft-versus-tumor activity. Blood. 2006; 108:2463–2469. [PubMed: 16757683]

33. Roychowdhury S, Blaser BW, Freud AG, Katz K, Bhatt D, Ferketich AK, Bergdall V, Kusewitt D, Baiocchi RA, Caligiuri MA. IL-15 but not IL-2 rapidly induces lethal xenogeneic graft-versus-host disease. Blood. 2005; 106:2433–2435. [PubMed: 15976176]

34. Cario G, Izraeli S, Teichert A, et al. High interleukin-15 expression characterizes childhood acute lymphoblastic leukemia with involvement of the CNS. J Clin Oncol. 2007; 25:4813–4820. [PubMed: 17947730]

35. Wu S, Fischer L, Gökbuget N, Schwartz S, Burmeister T, Notter M, Hoelzer D, Fuchs H, Blau IW, Hofmann WK, Thiel E. Expression of interleukin 15 in primary adult acute lymphoblastic leukemia. Cancer. 2010; 116:387–392. [PubMed: 19924795]

36. Nasilowska-Adamska B, Czyz A, Markiewicz M, Rzepecki P, Piatkowska-Jakubas B, Paluszewska M, et al. Mild chronic graft-versus-host disease may alleviate poor prognosis associated with FLT3 internal tandem duplication for adult acute myeloid leukemia following allogeneic stem cell transplantation with myeloablative conditioning in first complete remission: a retrospective study. Eur J Haematol. 2016; 96:236–244. [PubMed: 25912052]

37. Barnes BJ, Moore PA, Pitha PM. Virus-specific activation of a novel interferon regulatory factor, IRF-5, results in the induction of distinct interferon alpha genes. J Biol Chem. 2001; 276:23382–23390. [PubMed: 11303025]

38. Steinmann J, Bertz H, Wäsch R, Marks R, Zeiser R, Bogatyreva L, Finke J, Lübbert M. 5-Azacytidine and DLI can induce long-term remissions in AML patients relapsed after allograft. Bone Marrow Transplant. 2015; 50:690–695. [PubMed: 25774594]

39. Bejanyan N, Weisdorf DJ, Logan BR, Wang HL, Devine SM, de Lima M, Bunjes DW, Zhang MJ. Survival of patients with acute myeloid leukemia relapsing after allogeneic hematopoietic cell transplantation: a center for international blood and marrow transplant research study. Biol Blood Marrow Transplant. 2015; 21:454–459. [PubMed: 25460355]

40. Takami A, Yano S, Yokoyama H, Kuwatsuka Y, Yamaguchi T, Kanda Y, et al. Donor lymphocyte infusion for the treatment of relapsed acute myeloid leukemia after allogeneic hematopoietic stem cell transplantation: a retrospective analysis by the Adult Acute Myeloid Leukemia Working Group of the Japan Society for Hematopoietic Cell Transplantation. Biol Blood Marrow Transplant. 2014; 20:1785–1790. [PubMed: 25034960]

41. Buck MD, O'Sullivan D, Klein Geltink RI, Curtis JD, Chang CH, Sanin DE, Qiu J, Kretz O, Braas D, van der Windt GJ, Chen Q, Huang SC, O'Neill CM, Edelson BT, Pearce EJ, Sesaki H, Huber TB, Rambold AS, Pearce EL. Mitochondrial Dynamics Controls T Cell Fate through Metabolic Programming. Cell. 2016; 166:63–76. [PubMed: 27293185]

42. Bolger AM, Lohse M, Usadel B. Trimmomatic: a flexible trimmer for Illumina sequence data. Bioinformatics (Oxford, England). 2014; 30:2114–2120.

43. Li H, Durbin R. Fast and accurate long-read alignment with Burrows-Wheeler transform. Bioinformatics (Oxford, England). 2010; 26:589–595.

44. McKenna A, Hanna M, Banks E, Sivachenko A, Cibulskis K, Kernytsky A, Garimella K, Altshuler D, Gabriel S, Daly M, DePristo MA. The Genome Analysis Toolkit: a MapReduce framework for analyzing next-generation DNA sequencing data. Genome Res. 2010; 20:1297–1303. [PubMed: 20644199]

45. Lek M, et al. Analysis of protein-coding genetic variation in 60,706 humans. Nature. 2016; 536:285–291. [PubMed: 27535533]

46. Boeva V, Popova T, Bleakley K, Chiche P, Cappo J, Schleiermacher G, Janoueix-Lerosey I, Delattre O, Barillot E. Control-FREEC: a tool for assessing copy number and allelic content using next-generation sequencing data. Bioinformatics (Oxford, England). 2012; 28:423–425.

47. Carvalho BS, Irizarry RA. A framework for oligonucleotide microarray preprocessing. Bioinformatics (Oxford, England). 2010; 26:2363–2367.

48. Luo W, Friedman MS, Shedden K, Hankenson KD, Woolf PJ. GAGE: generally applicable gene set enrichment for pathway analysis. BMC Bioinformatics. 2009; 10:161. [PubMed: 19473525]

49. Kamburov A, Stelzl U, Lehrach H, Herwig R. The ConsensusPathDB interaction database: 2013 update. Nucleic Acids Res. 2013; 41:793–800.

50. Brummer T, Larance M, Herrera Abreu MT, Lyons RJ, Timpson P, Emmerich CH, Fleuren ED, Lehrbach GM, Schramek D, Guilhaus M, James DE, Daly RJ. Phosphorylation-dependent binding of 14-3-3 terminates signalling by the Gab2 docking protein. EMBO Journal. 2008; 27:2305–2316. [PubMed: 19172738]

51. Wilhelm K, Ganesan J, Müller T, Dürr C, Grimm M, Beilhack A, Krempl CD, Sorichter S, Gerlach UV, Jüttner E, Zerweck A, Gärtner F, Pellegatti P, Di Virgilio F, Ferrari D, Kambham N, Fisch P, Finke J, Idzko M, Zeiser R. Graft-versus-host disease enhanced by extracellular adenosine triphosphate activating P2X7R. Nature medicine. 2010; 12:1434–1438.

52. Schwab L, Goroncy L, Palaniyandi S, Gautam S, Triantafyllopoulou A, Mocsai A, Reichardt W, Karlsson FJ, Radhakrishnan SV, Hanke K, Schmitt-Graeff A, Freudenberg M, von Loewenich FD, Wolf P, Leonhardt F, Baxan N, Pfeifer D, Schmah O, Schönle A, Martin SF, Mertelsmann R, Duyster J, Finke J, Prinz M, Henneke P, Häcker H, Hildebrandt GC, Häcker G, Zeiser R. Neutrophil granulocytes recruited upon translocation of intestinal bacteria enhance GvHD via tissue damage. Nature medicine. 2014; 20:648–654.

53. Kaplan DH, Anderson BE, McNiff JM, Jain D, Shlomchik MJ, Shlomchik WD. Target antigens determine graft-versus-host disease phenotype. J Immunol. 2004; 173:5467–5475. [PubMed: 15494494]
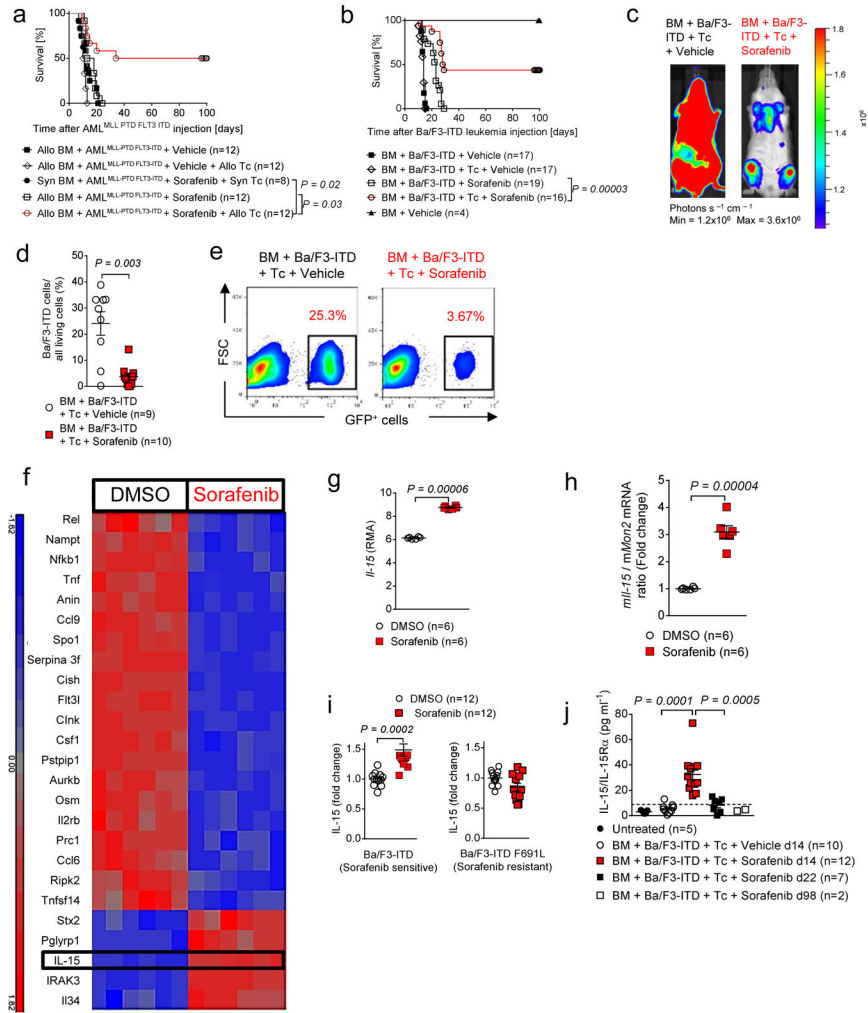
Figure 1. Sorafenib synergizes with allogeneic T-cells and improves survival in FLT3-ITD driven AML mouse models by increasing IL-15 production

(a) Percentage survival of C57BL/6 recipient mice receiving AML$^{MLL\text{-}PTD\ FLT3\text{-}ITD}$ cells (C57BL/6 background) and BALB/c BM or C57BL/6 BM (syn BM) with or without additional BALB/c T-cells (allo Tc) or C57BL/6 T-cells (syn Tc) and treated with either vehicle or sorafenib. The experiment was performed twice and the results were pooled; $n=12$ biologically independent animals per group are shown, except for the group Syn BM +AML$^{MLL\text{-}PTD\ FLT3\text{-}ITD}$+ Sorafenib+Syn Tc, here $n=8$ biologically independent animals per group are shown. P-values were calculated using the two-sided Mantel-Cox test.

(b) Percentage survival of BALB/c recipients receiving C57BL/6 BM and Ba/F3-ITD cells with or without additional C57BL/6 T-cells and treated with vehicle or sorafenib as described in (**a**). The experiment was performed three times and the results were pooled; BM+Ba/F3-ITD+Vehicle ($n=17$, biologically independent animals), BM+Ba/F3-ITD+Tc +Vehicle ($n=17$, biologically independent animals), BM+Ba/F3-ITD+Sorafenib ($n=19$, biologically independent animals), BM+Ba/F3-ITD+Tc+Sorafenib ($n=16$, biologically independent animals), BM+Vehicle ($n=4$, biologically independent animals). P-values were calculated using the two-sided Mantel-Cox test.

(c) Bioluminescence imaging (BLI) on day 10 after Ba/F3-ITD[luc] cell transplantation showing the expansion of Ba/F3-ITD[luc] cells in BALB/c recipients transplanted with C57BL/6 BM and Tc and, treated with vehicle or sorafenib. Shown are BLI images of a representative mouse from the 2 indicated groups.

(d, e) Percentages of Ba/F3-ITD cells in the spleens of BALB/c mice on day 14, transplanted with C57BL/6 BM and Ba/F3-ITD cells with additional C57BL/6 T-cells, and treated with vehicle or sorafenib. **(d)** Percentage of GFP[+]Ba/F3-ITD cells in the spleens from each group. The experiment was performed three times and the results (mean ± s.e.m) were pooled; Tc+Vehicle (n=9, biologically independent animals per group), Tc+Sorafenib (n=10, biologically independent animals per group). The P-values were calculated using the two-sided Student's unpaired t-test. **(e)** Representative flow cytometry plots showing the percentages of GFP[+]Ba/F3-ITD cells in the spleens of mice from each group. The data are representative of one experiment out of three independent experiments.

(f, g) Microarray-based analysis of the expression levels of genes in Ba/F3-ITD cells that were treated with sorafenib (10 nM) or DMSO alone for 24 hours. **(f)** Tile display for the 25 most significantly regulated genes indicated by Robust Multichip Average (RMA) signal values, n=6, biologically independent samples per group. **(g)** Scatter plot showing the RMA values of *Il-15* in Ba/F3-ITD cells, n=6, biologically independent samples per group. The P-values were calculated using two-sided Student's unpaired t-test.

(h) Quantification of *Il-15* mRNA (mean ± s.e.m.) by qPCR in Ba/F3-ITD cells treated with 10nM sorafenib/DMSO relative to *Mon2* mRNA. The experiment was performed three times and the results (mean ± s.e.m) were pooled, n=6 biologically independent samples per group. The P-values were calculated using the two-sided Student's unpaired t-test.

(i) The scatter plot shows the quantification of intracellular IL-15 (fold change of Mean Fluorescence Intensity (MFI) of IL-15 with respect to mean MFI of IL-15 from DMSO treated controls). As indicated Ba/F3-ITD cells (sorafenib sensitive) and Ba/F3-ITD F691L cells (harboring a FLT3 resistance mutation) were studied. The experiment was performed three times and the results (mean ± s.e.m.) were pooled; n=12 biologically independent samples per group, each data point represents a biologically independent sample. The P-values were calculated using the two-sided Student's unpaired t-test.

(j) Quantification of serum IL-15/IL-15Rα (mean ± s.e.m.) from naive BALB/c mice (n=5, biologically independent samples) or BALB/c recipients transplanted with C57BL/6 BM and Ba/F3-ITD cells with additional C57BL/6 T-cells and treated with vehicle (n=10, biologically independent samples) or sorafenib on day 14 (n=12, biologically independent samples) or day 22 (n=7, biologically independent samples) or day 98 (n=2, biologically independent samples) following Ba/F3-ITD cells injection. The dotted line represents the detection limit (4 pg/ml) of mouse IL-15/IL-15Rα ELISA. The experiment was repeated three times (except for the day 98 group) and the results (mean ± s.e.m.) were pooled. Each data point represents a biologically independent sample derived from an individual mouse. The P-values were calculated using a two-sided Mann-Whitney U test.
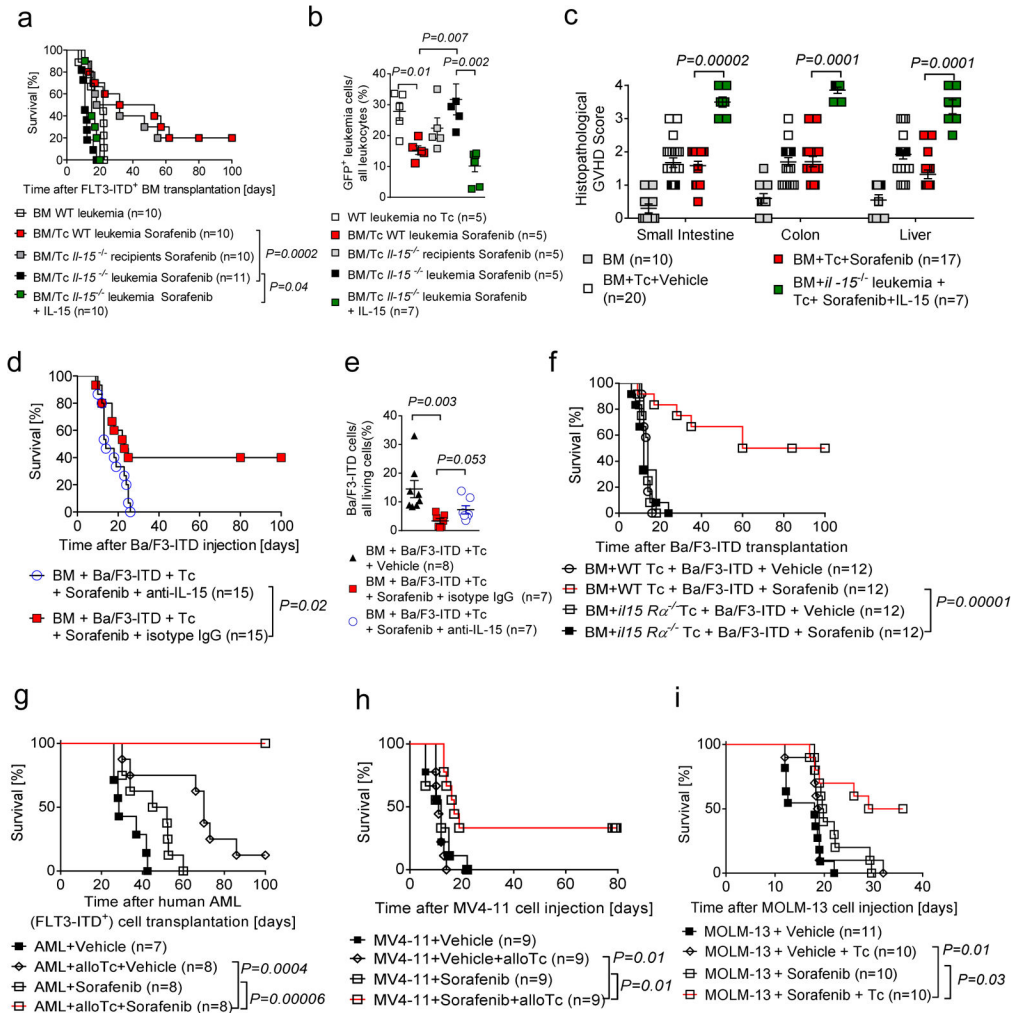
Figure 2. Sorafenib induced IL-15 production is derived from leukemia cells *in vivo* and synergizes with T cells in humanized mouse models

(a) The survival rate of C57BL/6 recipient mice is shown. Mice (C57BL/6) were transplanted with WT BALB/c BM, as well as with GFP$^+$FLT3-ITD$^+$ C57BL/6 BM to induce the leukemia. On day 2 T-cells (BALB/c) were given to induce the allogeneic immune effect. The GFP$^+$FLT3-ITD$^+$ BM was derived from either WT C57BL/6 mice (white open squares; WT leukemia no T-cells) (*n*=10, biologically independent animals) or from *Il-15$^{-/-}$* C57BL/6 mice to generate IL-15 deficient leukemia cells when indicated. In one group WT C57BL/6 recipients were transplanted with BALB/c BM, GFP$^+$FLT3-ITD$^+$ WT C57BL/6 BM and BALB/c T-cells and treated with sorafenib (red squares, BM/Tc WT leukemia sorafenib) (*n*=10, biologically independent animals). In another group *Il-15$^{-/-}$* C57BL/6 recipients were transplanted with BALB/c BM, FLT3-ITD$^+$ WT C57BL/6 BM and BALB/c T-cells and treated with sorafenib (grey squares BM/Tc *Il-15$^{-/-}$* recipients + sorafenib) (*n*=10, biologically independent animals). In another group WT C57BL/6 recipients were transplanted with BALB/c BM, GFP$^+$FLT3-ITD$^+$ *Il-15$^{-/-}$* C57BL/6 BM and BALB/c T-cells and treated with sorafenib (black squares; BM/Tc *Il-15$^{-/-}$* leukemia + sorafenib) (*n*=11, biologically independent animals). In an additional setting WT C57BL/6

recipients were transplanted with BALB/c BM, GFP⁺FLT3-ITD⁺ *Il-15^{−/−}* C57BL/6 BM and BALB/c T-cells, and treated with sorafenib and IL-15 (green squares; BM/Tc *Il-15^{−/−}* leukemia, sorafenib + IL-15) (*n*=10, biologically independent animals). Biologically independent animals per group are shown. The experiment was performed twice and the results were pooled. *P*-values were calculated using the two-sided Mantel-Cox test.

(b) Percentage of GFP⁺Ba/F3-ITD cells of all leukocytes in the blood of mice on day 14 from the groups described in **(a)**. The experiment was performed twice and the results (mean ± s.e.m) were pooled; WT leukemia no T-cells (*n*=5, biologically independent samples), BM/Tc WT leukemia + sorafenib (*n*=5, biologically independent samples), BM/Tc *Il-15^{−/−}* recipients + sorafenib (*n*=5, biologically independent samples), BM/Tc *Il-15^{−/−}* leukemia + sorafenib (*n*=5, biologically independent samples), BM/Tc *Il-15^{−/−}* leukemia + sorafenib + IL-15 (*n*=7, biologically independent samples). The *P*-values were calculated using the two-sided Mann-Whitney *U* test and are indicated in the graph.

(c) The scatter plot shows the histopathological scores from different GvHD target organs isolated on day 10 following allo-HCT of BALB/c mice transplanted with T-cells/vehicle or T-cells/sorafenib, or of C57BL/6 recipients transplanted with FLT3-ITD⁺ BM cells/T-cells/ sorafenib/IL-15. The experiment was performed twice and the results (mean ± s.e.m.) were pooled; BM (*n*=10, biologically independent samples), BM+Tc+vehicle (*n*=20, biologically independent samples), BM+Tc+sorafenib (*n*=17, biologically independent samples), BM +*il15^{−/−}* leukemia+Tc+sorafenib (*n*=7, biologically independent samples). The *P*-value was calculated using the two-sided Mann-Whitney *U* test; *P>0.05*, non-significant (*NS*).

(d) Percentage survival of BALB/c recipients receiving C57BL/6 BM and Ba/F3-ITD cells with additional C57BL/6 Tc and treated with sorafenib and non-specific IgG or anti-IL-15 antibody, as indicated for each group. The experiment was performed three times and the results were pooled, *n*=15 biologically independent animals per group. *P*-values were calculated using the two-sided Mantel-Cox test.

(e) Percentage of GFP⁺Ba/F3-ITD cells of all living cells in the spleens on day 14 of mice from the groups as described in **(d)** with an additional group which was treated with vehicle. The experiment was performed two times and the results (mean ± s.e.m) were pooled; Tc +Vehicle (*n*=8, biologically independent samples), Tc+Sorafenib+isotype IgG (*n*=7, biologically independent samples), Tc+Sorafenib+anti-IL-15 (*n*=7, biologically independent samples). The *P*-values were calculated using the two-sided Mann-Whitney *U* test. *P*-values are indicated in the graph.

(f) The survival rate of BALB/c recipients injected with Ba/F3-ITD cells is shown. Mice were transplanted with C57BL/6 WT BM (day 0) and on day 2 with additional C57BL/6 WT T-cells or *Il-15Ra^{−/−}* T-cells. The experiment was performed twice with similar results; *n*=12 biologically independent animals per group. Biologically independent animals per group are shown. *P*-values were calculated using the two-sided Mantel-Cox test.

(g) Percentage survival of *NSG* mice receiving primary human FLT3-ITD⁺ AML cells from a HLA-A2⁺ patient with additional allogeneic human CD8⁺ T-cells that had been stimulated and expanded in the presence of autologous DCs expressing allogeneic HLA-A2 upon RNA transfection *in vitro*. Mice were treated with vehicle or sorafenib as indicated. The experiment was performed twice with similar results; *n*=8 biologically independent animals per group except for AML+ Vehicle (*n*=7 biologically independent animals). Biologically

independent animals per group are shown. *P*-values were calculated using the two-sided Mantel-Cox test.

(h) Percentage survival of *Rag2*$^{-/-}$*Il2rγ*$^{-/-}$ recipient mice receiving human MV4-11 FLT3-ITD mutant) cells with or without additional C57BL/6 T-cells and being treated with vehicle or sorafenib. The experiment was performed three times and the results were pooled; *n*=9 biologically independent animals per group. Biologically independent animals per group are shown. *P*-values were calculated using the two-sided Mantel-Cox test.

(i) Percentage survival of *Rag2*$^{-/-}$*Il2rγ*$^{-/-}$ recipient mice receiving human MOLM-13 (FLT3-ITD mutant) cells with or without additional C57BL/6 T-cells and being treated with vehicle or sorafenib. The experiment was performed once, *n*=10 biologically independent animals per group. Biologically independent animals per group are shown. *P*-values were calculated using the two-sided Mantel-Cox test.
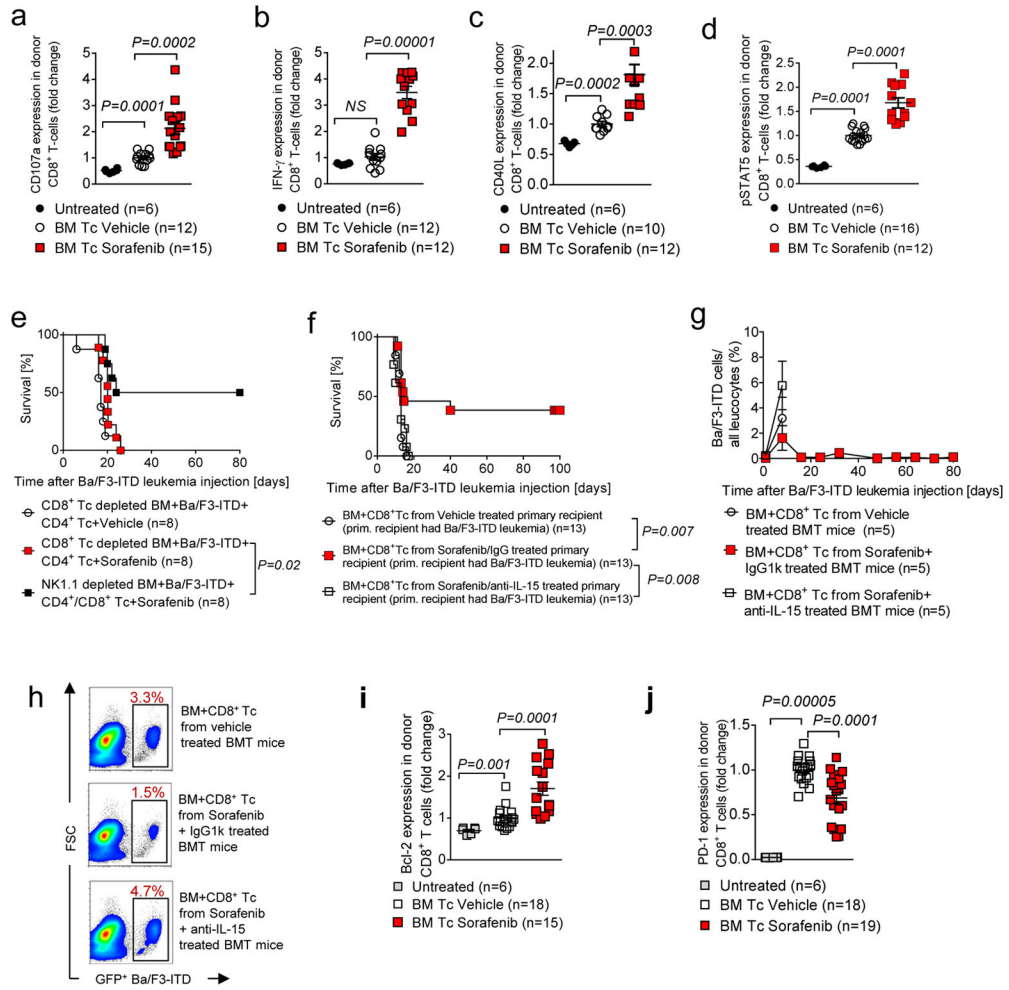
Figure 3. Sorafenib promotes cytotoxicity and longevity of donor CD8^{+} T-cells via IL-15

(a–d) Flow cytometry analysis of the spleens of BALB/c mice transplanted with C57BL/6 BM, Ba/F3-ITD cells (day 0) and T-cells (C57BL/6, day 2) as described in Figure 1b. The time point of analysis is day 12 following Ba/F3-ITD injection.

(a) Scatter plot showing the fold change of MFI (with respect to mean MFI of vehicle treated group) for CD107a of all living donor-derived (H-2kb^{+}) CD8^{+} T-cells from BMT recipients treated with vehicle (n=12, biologically independent samples) or sorafenib (n=15, biologically independent samples) or from untreated naive C57BL/6 mice (n=6, biologically independent samples) as indicated. The experiment was repeated three times and the results (mean ± s.e.m.) were pooled. The P-values were calculated using the two-sided Student's unpaired t-test.

(b) Scatter plot showing the fold change of MFI (with respect to mean MFI of vehicle treated group) for IFN-γ of all living donor-derived (H-2kb^{+}) CD8^{+} T-cells from BMT recipients treated with vehicle (n=12, biologically independent samples) or sorafenib (n=12, biologically independent samples) or from untreated naive C57BL/6 mice (n=6, biologically independent samples) as indicated. The experiment was done three times and the results (mean ± s.e.m.) were pooled. The P-values were calculated by two-sided Student's unpaired t-test; $P>0.05$, Not significant (*NS*).

(c) Scatter plot showing the fold change of MFI (with respect to mean MFI of vehicle treated group) for CD40L of all living donor-derived (H-2kb$^+$) CD8$^+$ T-cells from BMT recipients treated vehicle (n=10, biologically independent samples) or sorafenib (n=12, biologically independent samples) or from untreated naive C57BL/6 mice (n=6, biologically independent samples) as indicated. The experiment was repeated three times and the results (mean $\pm$ s.e.m.) were pooled. The P-values were calculated using a two-sided Student's unpaired t-test.

(d) Scatter plot showing the quantification of phospho-STAT5 expression levels (the fold change of MFI with respect to mean MFI of vehicle treated group) in all living donor-derived (H-2kb$^+$) CD8$^+$ T-cells from BMT recipients treated with vehicle (n=16, biologically independent samples) or sorafenib (n=12, biologically independent samples) or from untreated naive C57BL/6 mice (n=6, biologically independent samples) as indicated. Each data point represents an individual sample of one biologically independent animal. The experiment was repeated three times and the results (mean $\pm$ s.e.m.) were pooled. The P-values were calculated with the two-sided Student's unpaired t-test.

(e) Survival rate of BALB/c mice which received Ba/F3-ITD cells, CD8$^+$ Tc-depleted C57BL/6 BM and CD4$^+$ T-cells; or Ba/F3-ITD cells, NK1.1-depleted C57BL/6 BM and T-cells and being treated with either sorafenib or vehicle. The experiment was repeated twice and the results were pooled; n=8, biologically independent animals per group. Biologically independent animals per group are shown. P-values were calculated using the two-sided Mantel-Cox test.

(f) Survival rate of BALB/c mice ("secondary recipients") which received C57BL/6 BM (5×10^6), Ba/F3-ITD cells (day 0) and on day 2 H-2kb$^+$ CD3$^+$ CD8$^+$ T-cells from the spleens of BALB/c mice ("primary recipients" day 12 after their BMT) which had received C57BL/6 BM (5×10^6), T-cells (2×10^5), and Ba/F3-ITD cells and had been treated with either vehicle or sorafenib/isotype IgG or sorafenib/anti-IL-15 antibody. The experiment was repeated three times and the results were pooled; n=13, biologically independent animals per group. Biologically independent animals per group are shown. P-values were calculated using the two-sided Mantel-Cox test.

(g) The graph is showing GFP$^+$Ba/F3-ITD cells (as percentages of all leucocytes) measured by flow cytometry in the blood of the different groups as described in **(f)** at different time points following transplantation. The experiment was repeated twice and the results (mean $\pm$ s.e.m.) were pooled, n=5, biologically independent samples per group.

(h) A representative flow cytometry plot showing the percentage of GFP$^+$Ba/F3-ITD cells (of all leucocytes) in the spleen on day 8 following transplantation of GFP$^+$Ba/F3-ITD cells from different groups as described in **(f)**.

(i) Scatter plot showing the quantification of Bcl-2 expression levels (the fold change of MFI with respect to mean MFI of vehicle treated group) in all living donor-derived (H-2kb$^+$) CD8$^+$ T-cells from BMT recipients with Ba/F3-ITD cells and being treated with vehicle (n=18, biologically independent samples) or sorafenib (n=15, biologically independent samples) or from untreated naive C57BL/6 mice (n=6, biologically independent samples) as indicated. The experiment was repeated three times and the results (mean $\pm$ s.e.m.) were pooled. The P-values were calculated using the two-sided Mann-Whitney U test.

(j) Scatter plot showing the quantification for PD-1 expression (the fold change of MFI with respect to mean MFI of vehicle treated group) of all living donor-derived (H-2kb$^+$) CD8$^+$ T-

cells from BMT recipients treated with vehicle (n=18, biologically independent samples) or sorafenib (n=19, biologically independent samples) or from untreated naive C57BL/6 mice (n=6, biologically independent samples) as indicated. Each data point represents an individual sample of one biologically independent animal. The experiment was performed three times and the results (mean ± s.e.m.) were pooled. The P-values were calculated using a two-sided Student's unpaired t-test.
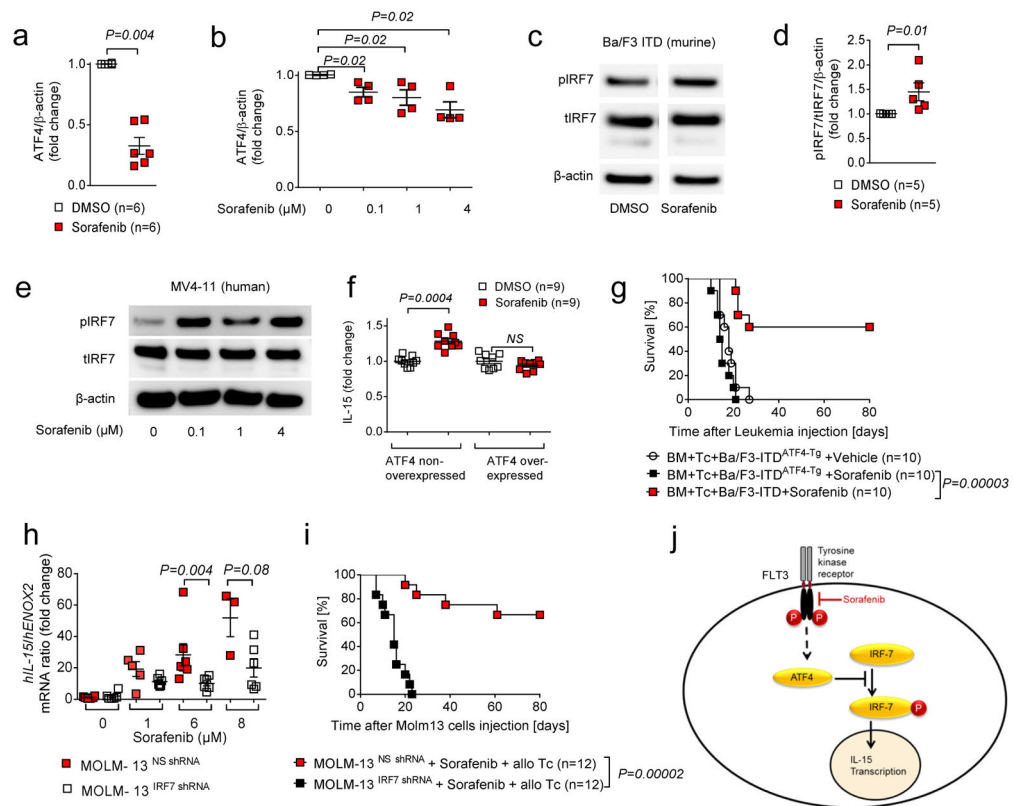
Figure 4. Sorafenib induces phosphorylation of IRF7 by reducing its inhibitor ATF4

(a, b) Quantification of ATF4 (western blot) normalized to β-actin (fold change with respect to DMSO treated controls) in mouse Ba/F3-ITD **(a)** or human FLT3-ITD mutant MV4-11 **(b)** leukemia cells exposed to sorafenib as indicated. The experiment was done three times and the results (mean ± s.e.m.) were pooled; a: n=6 biologically independent samples per group, b: n=4 biologically independent samples per group. The P-values were calculated using a two-sided Mann-Whitney U test.

(c) Western blots showing the expression of pIRF7, tIRF7 and loading control (β-actin) in Ba/F3-ITD cells exposed to sorafenib. Blot images were cropped and the pieces are separated by a white border. The uncut gels of all western blots are shown in Suppl. Fig.15–21.

(d) Quantification of pIRF7/tIRF7 normalized to β-actin (fold change with respect to DMSO treated controls) in Ba/F3-ITD cells treated as described. The experiment was repeated four times and the results (mean ± s.e.m.) were pooled, n=5 biologically independent samples per group. Each data point represents an individual sample of one independent cell culture experiment. The P-values were calculated using a two-sided Mann-Whitney U test.

(e) A representative Western blot showing the expression of pIRF7, tIRF7 and loading control (β-actin) in MV4-11 cells treated with the indicated sorafenib concentrations for 24 hours.

(f) Fold change of IL-15 (MFI) in Ba/F3-ITD cells or Ba/F3-ITD cells transfected with a lentiviral vector overexpressing mouse ATF4 and when indicated treated with sorafenib (0.1 μM) for 24 hours. n=9 biologically independent cell culture samples. Each data point

represents an individual sample of one independent cell culture experiment. The *P*-values were calculated by using a two-sided Mann-Whitney *U* test.

(g) Percentage survival of BALB/c recipients receiving C57BL/6 BM and ATF4-overexpressing or ATF4-wildtype Ba/F3-ITD cells (500 cells) with additional C57BL/6 Tc (Tc, 2×10^5 cells, given on day 2) and treated with vehicle or sorafenib. The experiment was performed twice and the results were pooled; *n*=10, biologically independent animals per group. *P*-values were calculated using the two-sided Mantel-Cox test.

(h) Quantification of *IL-15* mRNA by qPCR in MOLM-13 (human FLT3-ITD[+] AML cell line) cells containing a non-silencing vector (MOLM-13[NS shRNA]) or an IRF7 knockdown vector (MOLM-13[IRF7 shRNA]). The MOLM-13 cells were exposed to the indicated concentrations of sorafenib. The experiment was repeated twice and the results (mean ± s.e.m.) were pooled, *n*=6 biologically independent samples per group. The *P*-values were calculated using a two-sided Mann-Whitney *U* test.

(i) Percentage survival of *Rag2*^{−/−}*Il2rγ*^{−/−} recipient mice receiving MOLM-13[NS shRNA] and MOLM-13[IRF7 shRNA] as indicated. The experiment was performed twice and the results were pooled, *n*=12 biologically independent animals per group. *P*-values were calculated using a two-sided Mantel-Cox test.

(j) Proposed mechanism as to how sorafenib leads to increased IL-15 transcription. Sorafenib inhibits FLT3 receptor tyrosine kinase signaling which normally leads to ATF4 production. Reduced ATF4 levels lead to less inhibition of IRF7 phosphorylation and activation. Active pIRF7 can translocate to the nucleus where it activates IL-15 transcription.
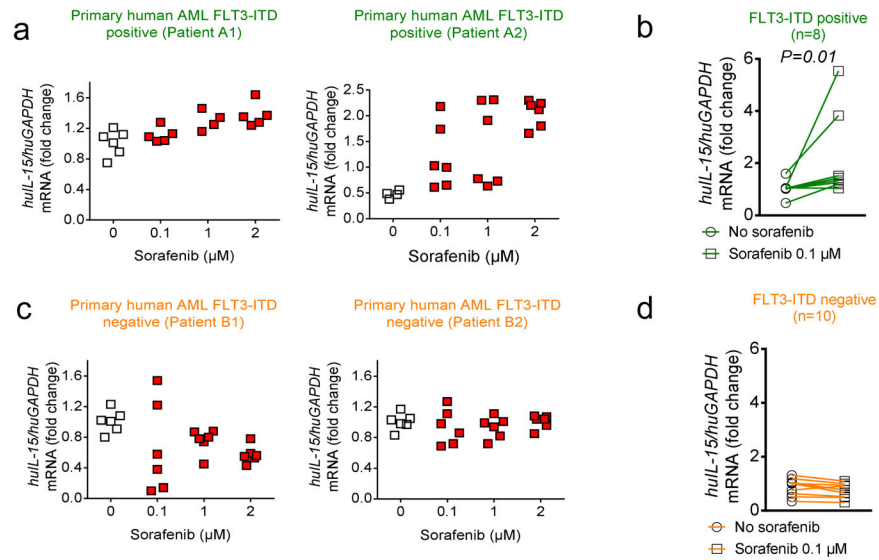
Figure 5. Treatment with sorafenib induces IL-15 in human primary FLT3-ITD+ leukemia cells

(a) Representative *IL-15* mRNA levels determined by qPCR within primary human AML FLT3-ITD+ cells. Six technical repeats from two independent patients per group are shown. Since these results display only representative data from technical replicates no statistical analysis was performed.

(b) Cumulative *IL-15* mRNA levels determined by qPCR within primary human AML FLT3-ITD+ cells (*n*=8, biologically independent patients) are displayed. Each data point indicates the *IL-15/GAPDH* mRNA ratio in the AML cells exposed to sorafenib or DMSO. *P*-values were calculated using the two-sided Wilcoxon matched-pairs signed rank test and are indicated in the graph.

(c) Representative *IL-15* mRNA levels determined by qPCR within primary human AML FLT3-ITDnegative cells. Six technical repeats from two independent patients per group are shown. Since these results display only representative data from technical replicates no statistical analysis was performed.

(d) Cumulative *IL-15* mRNA levels determined by qPCR within primary human AML FLT3-ITDnegative cells (*n*=10, biologically independent patients) are displayed. Each data point indicates the *IL-15/GAPDH* mRNA ratio in the AML cells exposed to sorafenib or DMSO. *P*-values were calculated using the two-sided Wilcoxon matched-pairs signed rank test and are indicated in the graph.

Figure 6. Treatment with sorafenib increases the frequency of T-cells that have active glycolysis in patients with FLT3-ITD$^+$ AML which relapse after allo-HCT

(a) IL-15 levels in the serum of patients relapsing with FLT3-ITD$^+$ AML after allo-HCT. Sorafenib/DLI responders (*n*=19 biologically independent patients) and non-responders (*n*=14, biologically independent patients) are shown separately. Each data point indicates the IL-15 level in the serum of a patient before sorafenib (So) treatment (day 0) and after start of sorafenib-treatment (day 3 after start of treatment and before the patients received donor lymphocyte infusions, DLI). The dotted line in the graph indicates the detection limit (4 pg/ml) of the IL-15 ELISA. The *P*-value was determined using the two-sided Wilcoxon matched-pairs signed rank test and is indicated in the graph.

(b) Quantification of *IL-15* mRNA expression by qPCR in leukemia cells (>90% purity) derived from the peripheral blood of FLT3-ITD$^+$ AML patients (responders *n*=14 biologically independent patients, non-responders, *n*=14 biologically independent patients) before (day -3) and day 6 after start of sorafenib-treatment. Each data point indicates the measurement of an individual patient at the indicated time point. The *P*-value was determined by using the two-sided Wilcoxon matched-pairs signed rank test.

(c) Quantification of pIRF7$^+$ cells/HPF in BM biopsies of FLT3-ITD$^+$ AML patients (responders *n*=12 biologically independent patients, non-responders, *n*=12 biologically independent patients) before (day 0) and during sorafenib-treatment (day 15 after start of treatment). Each data point indicates the measurement of an individual patient at the

indicated time point. The *P*-value was determined by using the two-sided Wilcoxon matched-pairs signed rank test.

(d) IFN-γ levels in the serum of patients relapsing with FLT3-ITD$^+$ AML after allo-HCT. Sorafenib/DLI responders (*n*=19, biologically independent patients) and non-responders (*n*=14, biologically independent patients) are shown separately. Each data point indicates the IFN-γ level in the serum of a patient before (day 0) and after start of sorafenib-treatment (day 3 after start of treatment and before the patients received donor lymphocyte infusions, DLI). Responders: IFN-γ (serum level) before versus after sorafenib, *P=0.007*. Non-responders: no significant difference before vs after sorafenib. The *P*-value was determined using the two-sided Wilcoxon matched-pairs signed rank test.

(e) The heatmap displays the significance in having a smaller number of germline and somatic mutations in chromatin states marked as Tx (strong transcription) or TxW (weak transcription) around the transcription start site (TSS) of various interferon genes for non-responders (*n*=4, biologically independent patients) versus responders (*n*=4, biologically independent patients). IRF genes were hierarchically clustered by their Euclidean distance using complete linkage algorithm. Significance in mutation frequency was calculated from an analysis of variance with posthoc Tukey's test. *P*-values for the comparison of the different IRFs for responders vs non-responders were as follows; IRF7 *P=0.0005*, IRF5: *P=0.001* (like *IRF7* the *IRF5* activation induces IFN-responses [37]), not significant for: *IRF1-IRF4, IRF6-IRF9*.

(f) ECAR rates of CD8$^+$ T-cells after FCCP exposure, derived from the peripheral blood of FLT3-ITD$^+$ AML patients (only responders *n*=12, biologically independent patients) before (day-2) and during sorafenib-treatment (day 4 after start of treatment). Each data point indicates the measurement of an individual patient at the indicated time point. The *P*-value was determined by using the two-sided Wilcoxon matched-pairs signed rank test.

(g) Change in OCR relative to basal level after FCCP exposure of CD8$^+$ T-cells, derived from the peripheral blood of FLT3-ITD$^+$ AML patients (only responders n=12, biologically independent patients) before (day-2) and during sorafenib-treatment (day 4 after start of treatment). Each data point indicates the measurement of an individual patient at the indicated time point. The *P*-value was determined by using the two-sided Wilcoxon matched-pairs signed rank test. Abbreviations: extracellular acidification rate (ECAR; reflecting the rate of glycolysis indicated by lactate secretion) and oxygen consumption rate (OCR; reflecting OXPHOS).

(h) ECAR rates of CD8$^+$ T-cells after FCCP exposure, derived from the peripheral blood of FLT3-ITD$^+$ AML patients (only non-responders n=14, biologically independent patients) before (day-2) and during sorafenib-treatment (day 4 after start of treatment). Each data point indicates the measurement of an individual patient at the indicated time point. The *P*-value was determined by using the two-sided Wilcoxon matched-pairs signed rank test.

(i) Change in OCR relative to basal level after FCCP exposure of CD8$^+$ T-cells, derived from the peripheral blood of FLT3-ITD$^+$ AML patients (only non-responders n=14, biologically independent patients) before (day-2) and during sorafenib-treatment (day 4 after start of treatment). Each data point indicates the measurement of an individual patient at the indicated time point. The *P*-value was determined by using the two-sided Wilcoxon matched-pairs signed rank test.

(j) Comparison of the median diversity index (DI) of TCR α and β complementarity determining region 3 (CDR3) amino acid sequences between responders and non-responders is shown. The analysis was performed on CD3^{+} cells isolated from responders (*n*=7, biologically independent patients) and non-responders (*n*=7, biologically independent patients) on day 30 after start of sorafenib. The *P*-value was determined by using the two-sided Mann-Whitney *U* test. No adjustments were made for multiple comparisons.